Journal of Autoimmunity 97 (2019) 88–99

Contents lists available at ScienceDirect

Journal of Autoimmunity

journal homepage: www.elsevier.com/locate/jautimm

Synaptotagmin-1 overexpression under inflammatory conditions affects secretion in salivary glands from Sjögren's syndrome patients

Juan Cortés[a], Jorge Hidalgo[b], Sergio Aguilera[c], Isabel Castro[d], Mónica Brito[a], Hery Urra[a], Paola Pérez[a], María-José Barrera[e], Patricia Carvajal[a], Ulises Urzúa[f], Sergio González[g], Claudio Molina[e], Verónica Bahamondes[d], Marcela Hermoso[h], María-Julieta González[a,*]

[a] Programa de Biología Celular y Molecular, Instituto de Ciencias Biomédicas, Facultad de Medicina, Universidad de Chile, Santiago, Chile
[b] Programa de Fisiología y Biofísica, Instituto de Ciencias Biomédicas, Facultad de Medicina, Universidad de Chile, Santiago, Chile
[c] Departamento de Reumatología, Clínica INDISA, Santiago, Chile
[d] Departamento de Tecnología Médica, Facultad de Medicina, Universidad de Chile, Santiago, Chile
[e] Facultad de Odontología, Universidad San Sebastián, Bellavista 7, Santiago, 8420524, Chile
[f] Departamento de Oncología Básico-Clínico, Facultad de Medicina, Universidad de Chile, Santiago, Chile
[g] Escuela de Odontología, Facultad de Ciencias, Universidad Mayor, Santiago, Chile
[h] Programa de Inmunología, Instituto de Ciencias Biomédicas, Facultad de Medicina, Universidad de Chile, Santiago, Chile

ARTICLE INFO

Keywords:
Synaptotagmin-1
PI(4,5)P_2
Ca^{2+} signaling
TNF-α
Salivary secretion
Sjögren's syndrome

ABSTRACT

Sjögren's syndrome (SS) is an autoimmune exocrinopathy associated with severe secretory alterations by disruption of the glandular architecture integrity, which is fundamental for a correct function and localization of the secretory machinery. Syt-1, PI(4,5)P_2 and Ca^{2+} are significant factors controlling exocytosis in different secretory cells, the Ca^{2+} role being the most studied. Salivary acinar cells from SS-patients show a defective agonist-regulated intracellular Ca^{2+} release together with a decreased IP3R expression level, and this condition may explain a reduced water release. However, there are not reports where Syt-1, PI(4,5)P_2 and Ca^{2+} in acinar cells of SS patients had been studied. In the present study, we analyzed the expression and/or localization of Syt-1 and PI(4,5)P_2 in acinar cells of labial salivary gland biopsies from SS-patients and control individuals. Also, we evaluated whether the overexpression of Syt-1 and the loss of cell polarity induced by TNF-α or loss of interaction between acinar cell and basal lamina, alters directionality of the exocytosis process, Ca^{2+} signaling and α-amylase secretion in a 3D-acini model stimulated with cholinergic or β-adrenergic agonists. In addition, the correlation between Syt-1 protein levels and clinical parameters was evaluated. The results showed an increase of Syt-1 mRNA and protein levels, and a high number of co-localization points of Syt-1/STX4 and PI(4,5)P_2/Ezrin in the acinar basolateral region of LSG from SS-patients. With regard to 3D-acini, Syt-1 overexpression increased exocytosis in the apical pole compared to control acini. TNF-α stimulation increased exocytic events in the basal pole, which was further enhanced by Syt-1 overexpression. Additionally, altered acinar cell polarity affected Ca^{2+} signaling and amylase secretion. Overexpression of Syt-1 was associated with salivary gland alterations revealing that the secretory dysfunction in SS-patients is linked to altered expression and/or localization of secretory machinery components together with impaired epithelial cell polarity. These findings provide a novel insight on the pathological mechanism implicated in ectopic secretory products to the extracellular matrix of LSG from SS-patients, which might initiate inflammation.

1. Introduction

Sjögren's syndrome (SS) is a systemic autoimmune disease that affects exocrine glands, mainly salivary and lacrimal, causing severe dysfunction with qualitative and quantitative changes in saliva components [1]. In salivary glands (SG) from SS-patients an initial intrinsic activation of the epithelial cells is followed by altered glandular homeostasis which precedes lymphocytic infiltration. This demonstrates that epithelial cells are active players in the gland inflammation by orchestrating the innate and adaptive immune responses [2] and

* Corresponding author. Programa de Biología Celular y Molecular, Instituto de Ciencias Biomédicas (ICBM), Facultad de Medicina, Universidad de Chile, Independencia 1027, Código postal 8380453, Santiago, Chile.
E-mail address: jgonzale@med.uchile.cl (M.-J. González).

https://doi.org/10.1016/j.jaut.2018.10.019
Received 31 August 2018; Received in revised form 19 October 2018; Accepted 22 October 2018
Available online 31 October 2018
0896-8411/

these alterations are associated to the inflammatory environment, where cytokines TNF-α and IFN-γ play a relevant role. In SS patients, both cytokines are synthesized and released by salivary gland epithelium and inflammatory infiltrate [3]. The acinar cells demonstrate changes in their structure due to altered expression, function and localization of protein involved in the secretory function [4]. For example, tight junction composition and organization is altered in salivary gland cells, which could be induced by TNF-α and IFN-γ [5], and cause disturbances in the directionality of the secretory process.

Apico-basal altered distribution of key proteins that participate in the fate of both mature secretory granules (Rab3D) and membrane fusion (SNARE) in regulated exocytosis were found in epithelial cells of salivary glands (SG) from SS patients [6,7]. Concomitant with the development of functional ectopic SNARE (fusion membrane receptors) complexes located mainly in the basolateral domain of acinar cells and are associated to an anomalous exocytosis of salivary mucins towards the extracellular matrix (ECM) of SG [7]. In turn, these ectopically located mucins activate the Toll-like receptor 4 pathway inducing cytokine expression thus generating a microenvironment contributing to the initiation and perpetuation of local autoimmune responses [8].

Regulated exocytosis is mediated by the SNARE complex, whose formation is chaperoned by several proteins and factors such as Synaptotagmin 1 (Syt-1), phosphatidylinositol 4,5-bisphosphate (PI(4,5)P_2) and Ca^{2+} which together achieve precise synchronicity of the secretory product release [9]. Syt-1 function is central in its role as primary Ca^{2+} sensor and is located in secretory granules acting as a link between Ca^{2+} stimulus and exocytic machinery components (v/tSNARE proteins) [9]. Within this context, we postulate that changes in epithelial cell polarity may also affect relevant components, such as Syt-1, PI(4,5)P_2 and Ca^{2+} in SG from SS patients.

Syt-1 is required for the rapid Ca^{2+}-triggered exocytosis, and as such Syt-1 is a Ca^{2+}-sensor whose intrinsic affinity for Ca^{2+} is quite low, but is also markedly enhanced by the interaction with SNAREs and PI(4,5)P_2. This interaction between the Syt-1/SNARE complex and Syt-1/PI(4,5)P_2 allows regulation of the fusion pore opening time [10] although, in resting conditions, Syt-1 is involved in pre-fusion docking of secretory granules to the plasma membrane through the interaction with the negatively charged PI(4,5)P2 in the plasma membrane [9]. Interestingly, Syt-1 was one of the most up-regulated genes in a microarray analysis performed with enriched epithelial cell fractions obtained from SS-patient labial salivary glands [11].

PI(4,5)P_2 promotes the interaction between Syt-1 and plasma membrane allowing exocytosis [12] and is concentrated at the apical region of 3D epithelial cell cultures promoting cell polarity [13]. At the same time, Ca^{2+} plays an important role in regulating exocytosis in polarized secretory cells, such as salivary acinar cells, where the Ca^{2+} signal starts from the apical pole and propagates to the basal pole [14]. In these cells, the increase in basal intracellular calcium concentration $[Ca^{2+}]_i$ and propagation of Ca^{2+} signal depends on Ca^{2+} released from the ER stores via inositol 1,4,5-trisphosphate receptors (InsP(3)R) as well as extracellular Ca^{2+} influx [14]. The reduction of $[Ca^{2+}]_i$ toward resting levels is accomplished by the activity of Ca^{2+}-ATPases localized to both the endoplasmic reticulum (ER) (SERCA-type pump) and the plasma membrane (PMCA-type pump) [15]. Increased intracellular Ca^{2+} levels are sensed by Syt-1 which in parallel modulates its binding to PI(4,5)P2 clusters located in apical plasma membrane microdomains. Thus, this decreases the electrostatic repulsion between both membranes, secretory granules and plasma membrane, and favours the formation of local fusion complexes by SNARE proteins [16].

Studies have demonstrated that Syt-1, PI(4,5)P_2 and Ca^{2+} are significant factors that control the exocytosis process in different secretory cells [17], the Ca^{2+} role being the most studied [18]. Salivary acinar cells from SS patients show a defective agonist-regulated intracellular Ca^{2+} release together with a decreased IP3R expression level, and this condition may explain the decrease of water release [19]. The authors also observed that key proteins such STIM1, IP3R, and AQP5, are altered within, or immediately around the area of lymphocytic infiltration where there is considerable tissue damage, while only IP3Rs are significantly decreased in the relatively intact areas of the gland where there is no infiltration [19]. However, there are not reports where Syt-1, PI(4,5)P_2 and Ca^{2+} in acinar cells of SS patients had been studied.

In the current study, we analyzed the expression and/or localization of Syt-1 and PI(4,5)P_2 in SG of SS patients. Also, we investigated how the over-expression of Syt-1 and changes in cell polarity induced by TNF-α stimulation or loss of interaction between cell and basal lamina alters the directionality of the exocytosis process and thus Ca^{2+} signaling together with α-amylase secretion in a 3D acini model.

Table 1
Demographic and serological characteristics of the SS-patient and control groups.

	Control subjects	Patients with primary Sjögren's syndrome
Numbers of individuals	21	23
Sex, no. female/no. male	21/0	22/1
Age, mean (range), years	41.3 (20–59)	47.1(27–64)
Xerophtalmia, nº (%)	4 (19%)	22 (95.6%)
Xerostomia, nº (%)	6 (28.6%)	21 (91.3%)
Focus score[a]		
1	0	3
2	0	9
3	0	5
≥4	0	6
USWSF, mean ± SD mL/15 min	2.73 ± 1.62	1.35 ± 1.38
Scintigraphic data score[b]		
1	1	0
2	10	3
3	10	3
4	0	17
Ro antibodies	0/21	20/23
Ro/La antibodies	0/21	11/23
Antinuclear antibodies (ANA)	2/21	20/23
Rheumatoid factor (RF)	0/21	11/23
ESSDAI, median (range)	–	6 (1–17)

USWSF: Unstimulated whole salivary flow, SD: standard deviation, nº: number, %: percentage, ESSDAI: EULAR Sjögren syndrome disease activity index; EULAR, European League against Rheumatism.

[a] Number of foci/4 mm^2 of tissue.

[b] 1 = normal salivary gland function, 2 = mild impairment of salivary gland function, 3 = moderate impairment of salivary gland function, and 4 = severe impairment of salivary gland function.

2. Materials and methods

2.1. Patients and controls

The study group included 23 SS patients and 21 control subjects (Table 1). Control subjects did not fulfill the primary SS classification criteria, were negative for anti-Ro and anti-La antibodies. They did not have systemic diseases and lip biopsy revealed no focal infiltration and eventually a mild diffuse chronic sialodenitis. The SS patients were diagnosed according to the American-European Consensus Group criteria [20]. All subjects signed an informed consent form following guidelines established by the Ethics Committee of the Faculty of Medicine, University of Chile.

2.2. Biopsy samples

LSG specimens were obtained as previously described [21]. Following surgery, samples were divided into 2 portions. One portion was snap frozen in liquid nitrogen and stored at −80 °C to extract RNA and proteins; the other was processed for a histological examination and

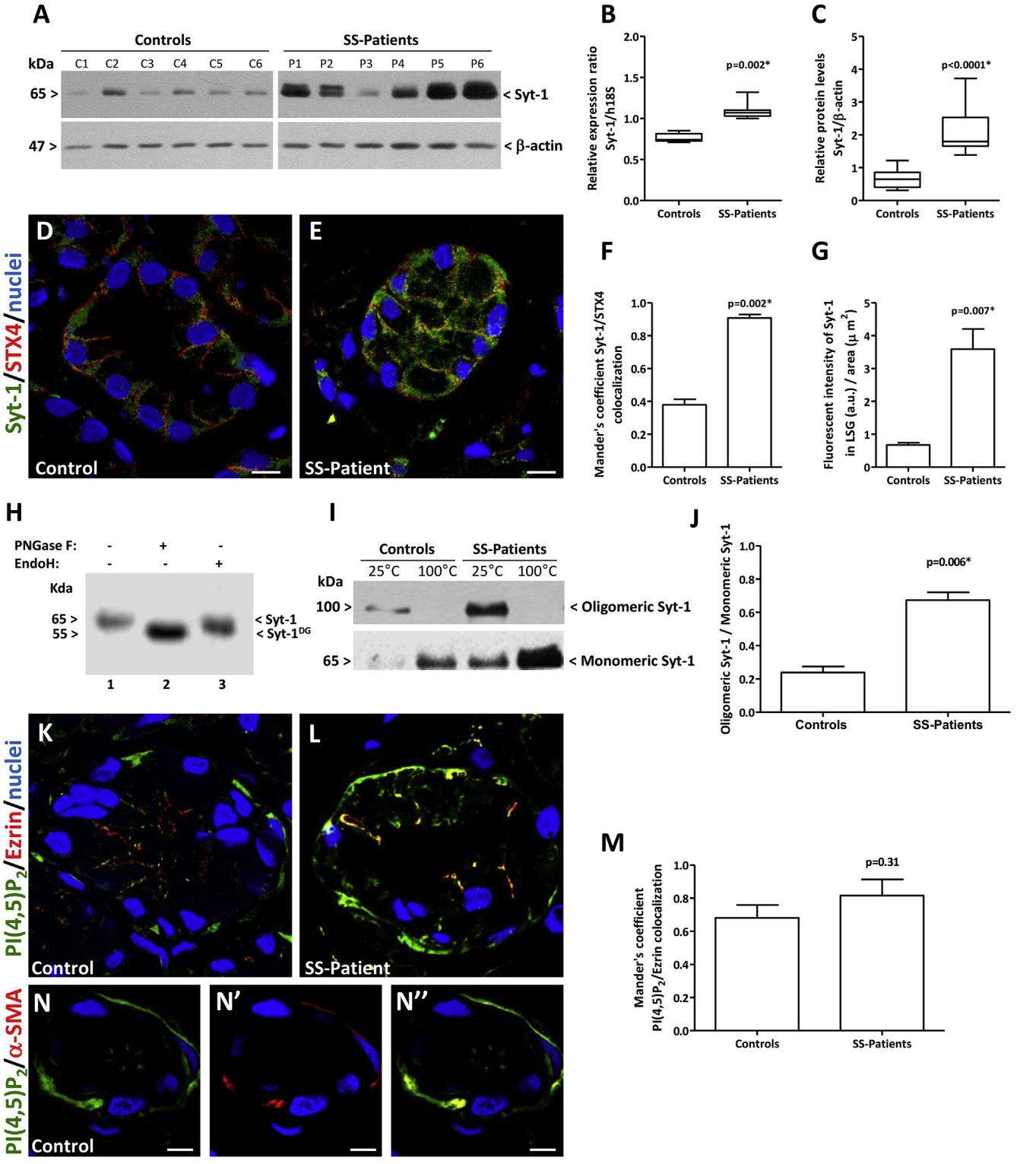

Fig. 1. Increased levels of Syt-1 in LSG from SS-patients. **A**, representative Western blot of LSG protein extracts from SS-patients (P) and controls (C) showing bands of 65 kDa for Syt-1 and 47 kDa for β-actin. **B**, box plot showing relative Syt-1 transcript levels using h18S as reference control. **C**, box plot showing relative Syt-1 protein levels normalized with β-actin. **D-E**, representative confocal image of a double staining of Syt-1 (green) and STX4 (red) in sections of LSG from controls and SS-patients, bars: 10 μm. **F**, colocalization of Syt-1/STX4 in sections of LSG from controls and SS-patients. **G**, staining intensity of Syt-1 in sections of LSG from controls and SS-patients, a. u. arbitrary units. **H,** N-glycosylation status of Syt-1 was confirmed by deglycosylation (DG) using PNGase F and EndoH in LSG extracts and subsequent detection of Syt-1 by western blotting. Lane 1: protein lysate, lane 2: PNGase-digested protein lysate, lane 3: EndoH-digested protein lysate. **I**, SDS-resistant oligomeric Syt-1 complexes show a 100 kDa band, while monomeric Syt-1 shows a 65 kDa band. **J**, oligomeric over monomeric Syt-1 ratio. **K-L**, representative confocal image of $PI(4,5)P_2$ (green) and Ezrin (red) double staining in LSG sections from controls and SS-patients, bars: 10 μm. **M**, colocalization of PI $(4,5)P_2$/Ezrin in LSG sections from controls and SS-patients. **N**, representative confocal image showing $PI(4,5)P_2$ (green) in the apical membrane of acinar cells and in the basal region of the acinus. **N′**, staining of α-smooth muscle actin (red) showed a distribution in the basal region of the acinus, marking myoepithelial cells. **N″**, the merge of the green and red channels showed colocalization of both marks in the myoepithelial cells. Bars: 10 μm. (*) $p < 0.05$ was considered significant. (For interpretation of the references to colour in this figure legend, the reader is referred to the Web version of this article.)

Table 2
Correlation coefficients between Syt-1 protein levels and clinical parameters of SS-patients.

	Age	Dryness		USWSF	Scintigraphy	Serology				Focus score	ESSDAI
		Eye	Mouth			Ro	La	RF	ANA		
Relative Syt-1 protein levels	0.2	0.67*	0.62*	−0.65*	0.56*	0.76**	0.62*	0.54*	0.81**	0.73*	0.86**

USWSF: Unstimulated whole salivary flow; for scintigraphic data we used lower values to indicate better glandular function. ESSDAI: EULAR Sjögren's syndrome disease activity index; EULAR, European League against Rheumatism.(*)$P < 0.05$; (**)$P < 0.0001$.

immunofluorescence.

2.3. 3D acini culture

3D acini were obtained by seeding human submandibular gland (HSG) cells on growth factor-reduced Matrigel (BD Biosciences, San Jose, CA, EEUU), as previously described [22]. Differentiated 3D acini were incubated with or without 1 or 10 ng/mL human recombinant TNF-α or 5 μg/mL rat monoclonal antibody against the α6 integrin subunit (GoH3) in serum free medium for 24 h.

2.4. Transfection

HSG cells were plated on a 10 cm plastic culture dish until 60–70% confluence and transfected with the DNA plasmids encoding EGFP (pEGFP-C1; Clontech) or Syt-1-GFP (pCMV6-Syt I-GFP; Origene, RG208938) with ViaFect Transfection Reagent (Promega) according to the manufacturer's instructions. At 20 h post-transfection, the medium was changed to DMEM F-12, supplemented with 5% FBS (Hyclon), 100 U/ml penicillin, and 100 μg/mL streptomycin. After 24 h, transfected HSG cells were seeded on BME to obtain 3D acini as previously described [22].

2.5. Real-time RT-PCR analysis

Total RNA was obtained from LSG using RNeasy Mini Kit (Qiagen), yield and purity of RNA were evaluated as previously described [23]. For PCR reaction we used Brilliant II SYBR Green qPCR Master Mix kit (Stratagene, CA, EEUU) and MxPro-MX 3000P thermocycler (Agilent Technologies, CA, EEUU). Template cDNA was obtained by reverse transcription of 1 μg total RNA with SuperScript II Reverse Transcriptase kit (Invitrogen, CA, EEUU). The relative transcript levels of Syt-1 or SERCA2b were expressed in comparison to h18S transcript levels using the efficiency-calibrated model [24].

2.6. Protein extraction and western blot

LSG specimens and 2D HSG cells were homogenized in RIPA buffer in the presence of Complete™ Protease Inhibitor Cocktail EDTA-free Mini Tablets (Roche, Mannheim, Germany) at 4 °C. The protein concentration of extracts was determined by the Bradford method [25]. 3D acini were detached from the matrigel with a Cultrex® 3D Culture Cell Harvesting kit (Trevigen Inc, Gaithersburg, MD, EEUU) according to the manufacturer's instructions and then homogenized in RIPA buffer with protease inhibitors. Total protein extracts (15–25 μg) were separated according to their molecular weights by SDS-PAGE on 8% gels under reducing conditions. The separated proteins were electro transferred to a nitrocellulose membrane (Bio-Rad Laboratories, Hercules, CA, EEUU). The membranes were probed with mouse anti-Syt-1 (1:3000, BD Biosciences), mouse anti-SERCA2b (1:3000, Thermo Scientific) or mouse anti-β-actin antibodies (1:20000, MP Biomedicals) and then incubated with goat anti-mouse, HRP-conjugated secondary antibodies (Jackson InmunoResearch Laboratories, Inc., PA, EEUU). Immunoreactive bands were visualized by chemiluminescence (Pierce, IL) and intensity of immunoreactive bands was quantified using the UNI-SCAN-IT (gel version for Windows 4.1, Silk Scientific, Orem, Utah, EEUU). Protein levels were normalized to β-actin.

2.7. Glycosylation state of Syt-1

Proteins (20 μg) of LSG were denatured in 10X glycoprotein denature buffer for 10 min at 100 °C and incubated for 1 h at 37 °C with PNGase F or EndoH in a total volume of 20 μL according to manufacturer instructions (New England BioLabs Inc., MA, USA). Control reactions included proteins treated under the same experimental conditions but in the absence of glycosidases. Samples were then mixed with sample buffer and boiled. Glycan removal was detected as a mobility shift using SDS-PAGE in 8% gels followed by Western blotting with anti-Syt-1 antibody.

2.8. Detection of SDS-resistant Syt-1 oligomers in LSG acinar cells

Syt-1 has been hypothesized as functioning in an oligomerized state during neurotransmitter release [26]. Consistent with this, Syt-1 form a stable SDS-resistant, β-mercaptoethanol-insensitive, and Ca^{2+}-independent oligomer surrounding the transmembrane domain [26]. The detection of SDS-resistant Syt-1 oligomers was performed as previously described [7]. Briefly, some aliquots of proteins were maintained at room temperature (RT, 25 °C) and others were boiled for 3 min at 100 °C to disassemble Syt-1 oligomers. The protein concentration of extracts was determined by the bicinchoninic acid (BCA) method [27].

2.9. Immunofluorescence

Tissue samples of LSGs were fixed in 1% paraformaldehyde for 6 h and paraffin embedded using standard procedures. Antigens were recovered by incubating the slides in 0.01 M citrate buffer (pH 6.0) for 25 min at 92 °C. The sections were blocked for 1 h at RT with 0.25% casein in PBS, pH7.4. To detect Syt-1 and STX-4, the tissues were incubated overnight at 4 °C with rabbit anti-Syt-1 (Cell Signaling, diluted 1:50 in PBS) and mouse anti-STX-4 (BD Biosciences, diluted 1:30 in PBS). Frozen tissue sections to detect $PI(4,5)P_2$ were fixed in 2% paraformaldehyde in buffer 5X (50 mM PIPES, [pH 7.0], 25 mM KCl, 1 mM $MgSO_4$, 45 mM NaCl, 2 mM $CaCl_2$, 10 mL PBS 10X, 0.5 M EDTA, [pH 7.0]) for 15 min. The frozen tissues were incubated in 100 mM glycine for 5 min, washed once with PBS 1X, and blocked for 1 h with 3% BSA. Slides were then incubated overnight at 4 °C with mouse anti-PI(4,5)P2, clone 2C11 (Life Technology, diluted 1:50 in PBS). 3D acini were fixed using 2% paraformaldehyde for 10 min, then washed and permeabilized with 0.2% Triton X-100 and incubated in 100 mM glycine twice for 5 min. The unspecific binding sites were blocked with 5% albumin in buffer IFI (0.2% Triton X-100, 0.5% Tween 20, 7.7 mM azide [pH 6.5], PBS 10X) for 1 h. The 3D acini were incubated overnight at 4 °C with mouse anti-Syt-1 (1:100, Cell Signaling), rabbit anti-Giantin (1:500, Covance) or rabbit anti-α-amylase (1:250) antibodies in blocking buffer. All slides and 3D acini were incubated at RT for 1 h with Alexa Fluor 488- or 546-conjugated secondary antibodies and Hoechst 33342, then mounted with Mowiol (Calbichem). As a negative control, rabbit Ig or mouse IgG fractions were employed (DakoCytomation, Inc., Carpinteria, CA, EEUU).

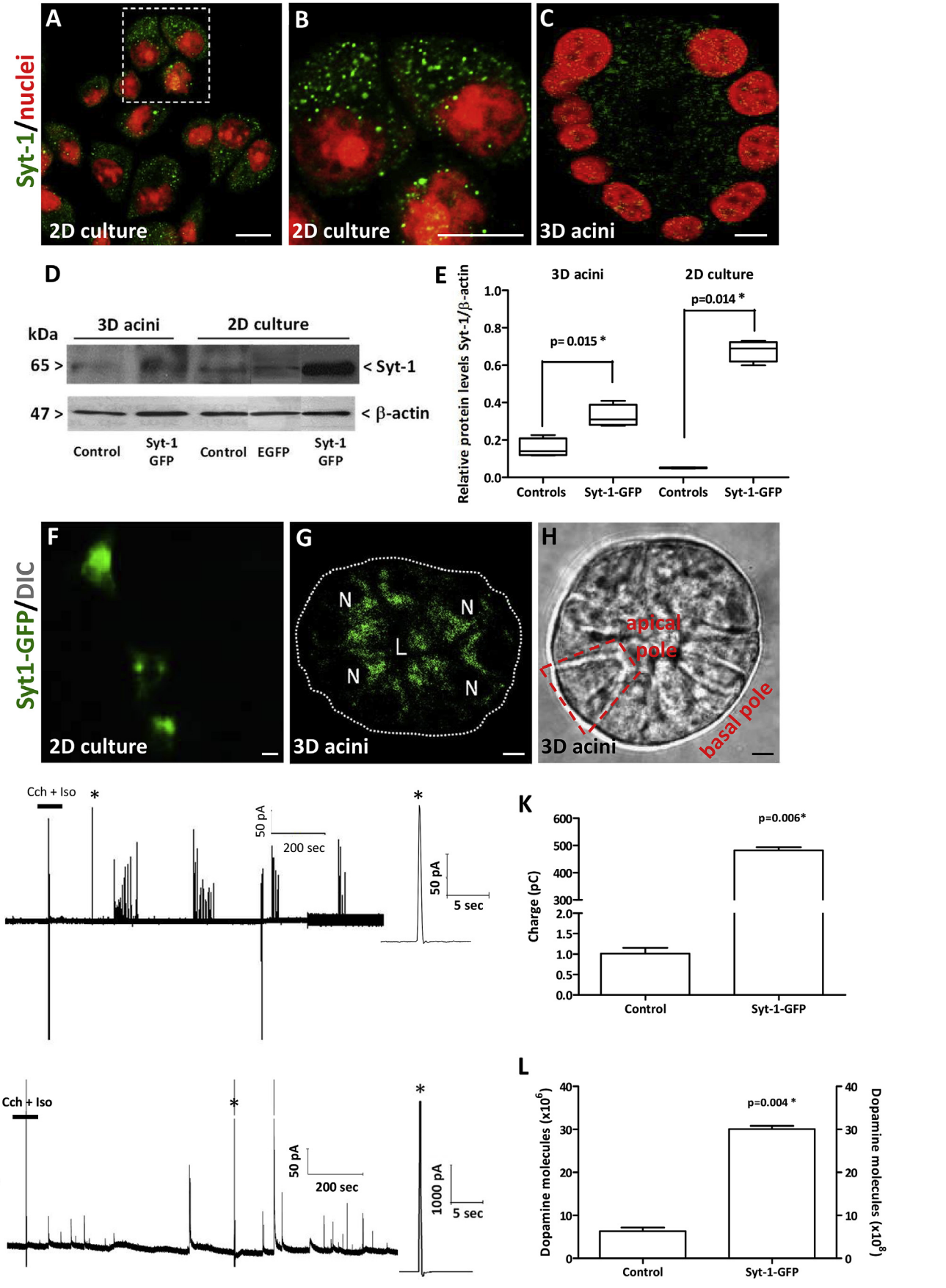

(caption on next page)

Fig. 2. Syt-1 overexpression increases exocytosis in the apical pole of 3D acini. A-C, immunofluorescence of endogenous Syt-1 (green) detection in 2D culture cells and 3D acini, bars: 10 μm. **D**, representative Western blot showing Syt-1 protein levels in extracts of 3D acini and 2D culture cells transfected with control EGFP or Syt-1-GFP plasmid. **E**, box plot showing relative Syt-1 protein levels in 3D acini and 2D culture cells transfected with Syt-1-GFP plasmid. **F-G**, representative confocal images of GFP in 2D culture cells and 3D acini transfected with Syt-1-GFP plasmid. **H**, representative DIC microscopy image of a 3D acinus showing the apical and basal poles where the carbon electrodes were placed for electrophysiological recordings. A single acinar cell with a truncated pyramidal shape is depicted with dashed lines. **I-J**, amperometric recordings in the apical pole of control or Syt-1-GFP transfected 3D acini, quantal events indicated with asterisks are shown with higher time resolution. **K**, total charge calculated from the integral of averaged amperometric currents in control or Syt-1-GFP transfected 3D acini. **L**, number of dopamine molecules released in the apical pole by control or Syt-1-GFP transfected 3D acini. (*) $p < 0.05$ was considered significant. (For interpretation of the references to colour in this figure legend, the reader is referred to the Web version of this article.)

2.10. Confocal microscopy and image analysis

All slides and 3D acini were visualized with an Olympus FluoView FV10i confocal laser scanning microscope (Olympus, EEUU). High-resolution digital images were captured and stored in TIFF format. The colocalization of signals from two channels was evaluated using the ImarisColoc module (Bitplane AG, Zurich, Switzerland). The degree of channel colocalization was analyzed considering the percentage of dataset colocalized and thresholded Manders's coefficient.

2.11. Measurement of $[Ca^{2+}]_i$

3D acini were cultured in glass-bottom microwell dishes, washed in PBS and loaded with 5 mM Fluo-4 acetoxymethyl ester (Molecular Probes, Invitrogen) in saline buffer (140 mM NaCl, 1 mM $MgCl_2$, 5 mM KCl, 1 mM $CaCl_2$, 5 mM glucose and 10 mM HEPES pH: 7.4) for 30 min at 37 °C. After loading, the cells were washed with saline buffer for 5 min. The dishes were mounted on an inverted fluorescence microscope (Zeiss Axiovert 200) and perfused with saline buffer at a rate of 1 mL/min at RT. For measurements in the absence of extracellular Ca^{2+}, cells were washed one time in nominally Ca^{2+}-free saline buffer supplemented with 2 mM $MgCl_2$. Fluo-4 confocal fluorescence images were obtained with a LSM5 Pascal (Zeiss) scanner attached to the microscope. Images from regions of interest were captured every 10 s with a 60X oil immersion objective. For converting fluorescence data into $[Ca^{2+}]$, we determined minimum and maximum Fluo-4 fluorescence data using the following equation:

$$[Ca^{2+}] = \frac{kd(F-F_{min})}{(F_{max}-F)}$$

2.12. Amperometry

To record the release of dopamine by amperometry, 3D acini were loaded with dopamine for 45 min at 37 °C using a solution of 70 mM dopamine, 68 mM NaCl, 5 mM KCl, 1 mM $MgCl_2$, 1 mM $CaCl_2$, and 10 mM glucose in 10 mM HEPES pH 7.3. After loading, the cells were washed for 5 min and incubated for 4 h at 37 °C in DMEM F-12, supplemented with 10% FBS (Hyclon), 100 U/ml penicillin, and 100 μg/mL streptomycin. 3D acini were then placed in the normal recording saline buffer (140 mM NaCl, 5 mM KCl, 1 mM $MgCl_2$, 1 mM $CaCl_2$, and 10 mM glucose in 10 nM HEPES, pH 7.3). Dopamine release was recorded with an Axopatch 200B using a 5-μm carbon fiber electrode held at +660 mV compared to an Ag-AgCl electrode placed in the bath. 10 μM Carbachol (Cch) and 10 μM Isoproterenol (Iso) were used to stimulate and evoke secretion. To evaluate the release of endogenous amylase 3D acini were incubated with 6.5 mM 4-aminophenyl α-maltopentaoside (4AP-G_5), 12.5 U/mL α-glucosidase and 10 μM Cch and/or 10 μM Iso. A carbon electrode was held at +150 mV to detect current changes by electrochemical oxidation of 4AP, which is produced by the enzymatic action of endogenous amylase on 4AP-G_5 after secretagogue stimulation. After endogenous amylase recordings, exogenous α-amylase was added as an enzymatic positive control [28].

2.13. Statistical analysis

All values were processed to calculate their mean ± SD of at least 3 experiments. Statistical significance was determined by Mann-Whitney non-parametric test. Spearman rank correlation analysis was also performed. $P < 0.05$ was considered statistically significant.

3. Results

3.1. Increased levels of Syt-1 in LSG from SS-patients

Syt-1 is a Ca^{2+}-sensor protein that participates in the formation of the fusion pore between secretory granules (v-SNARE) and plasma membrane (t-SNAREs) [29]. Previous studies in LSG of SS-patients have shown altered protein and mRNA levels of SNARE proteins such as VAMP8, STX4 and STX3 [7]. Here, we compared the mRNA and protein levels of Syt-1 in LSG of 15 SS-patients and 12 control individuals, with results showing an increase of Syt-1 mRNA and protein levels ($p = 0.002$ and $p < 0.0001$, respectively) (Fig. 1A, B and 1C). It should be noted that in SS-patients a band with lower electrophoretic mobility was observed, which correspond to changes in Syt-1 N-glycosylation state (Fig. 1H). Syt-1 protein levels correlated inversely with unstimulated whole salivary flow and positively with symptoms of eye and mouth dryness, scintigraphy, presence of autoantibodies, focus score and ESSDAI (Table 2). Additionally, we compared the levels of SERCA2b, with results showing a decrease of mRNA and protein ($p = 0.002$ and $p = 0.02$, respectively) in LSG from SS-patients (Supplementary Fig. 1A, 1B and 1C).

The efficiency of the exocytic process in epithelial cells depends on the coordinated action of several components, for example the local concurrence of RabGTPase, $PI(4,5)P_2$, Ca^{2+}, Syt-1 and SNARE proteins [16]. Altered localization of SNARE proteins in LSG from SS-patients [7] suggests that the localization of Syt-1 could also be altered. Thus, we evaluated the co-localization of Syt-1 with STX4, showing more co-localization points in the basolateral region of LSG from SS-patients than controls ($p = 0.002$) (Fig. 1 and E, F). Similar to Western blot results, the Syt-1 fluorescence intensity was higher in SS-patients compared to controls ($p = 0.007$) (Fig. 1G).

When LSG protein extracts containing SDS were placed at 25 °C, a band near 100 kDa was observed for Syt-1, while a 65 kDa band was observed when protein extracts were placed at 100 °C. The 100/65 kDa ratio was higher in SS-patients compared with control subjects ($p = 0.006$) (Fig. 1I and J).

$PI(4,5)P_2$ recruits apical proteins, such as Ezrin, promoting the plasma membrane asymmetry [13]. A redistribution of Ezrin from the apical to the baso-lateral pole of epithelial cells has been observed in LSG from SS-patients [30]. Here, the $PI(4,5)P_2$/Ezrin double staining showed that both molecules are co-localized in the luminal region of epithelial cells of control LSG (Fig. 1K and M), whereas in LSG from SS-patients, they were found co-localizing mostly in the basolateral membrane (Fig. 1L and M). Interestingly, an intense green staining was observed in the plasma membrane of acinar and myoepithelial cells, the latter revealed by the colocalization of $PI(4,5)P_2$ with α-smooth muscle actin (α-SMA), a myoepithelial cell marker (Fig. 1N).

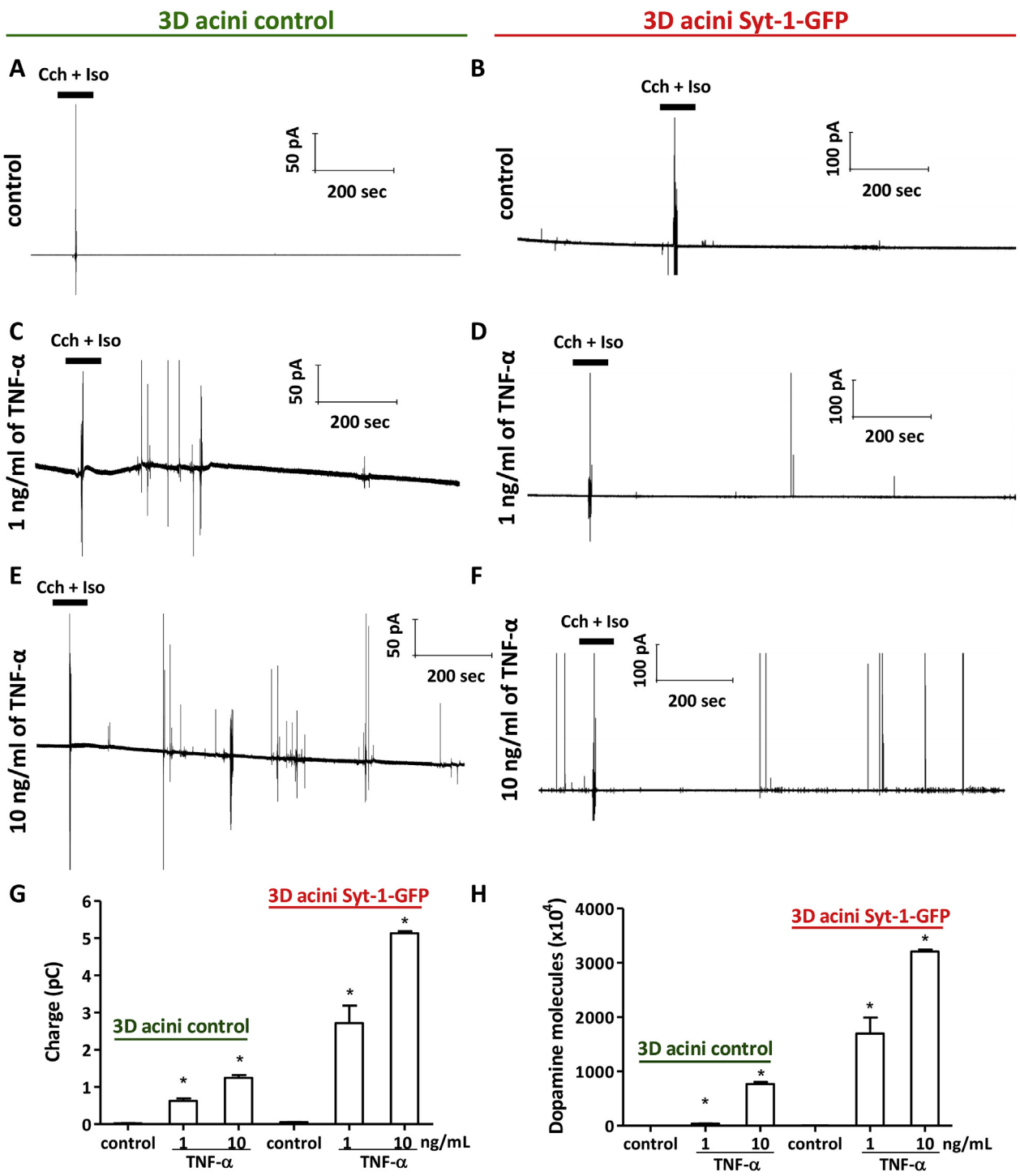

Fig. 3. TNF-α stimulation increases exocytic events in the basal pole, which is further enhanced by Syt-1 overexpression. A-C, amperometric exocytosis recordings from the basal pole of 3D acini control incubated with 0 (control), 1 or 10 ng/mL TNF-α for 24 h. **D-F**, amperometric exocytosis recordings from the basal pole of 3D acini overexpressing Syt-1 (3D acini Syt-1-GFP), incubated with 0, 1 or 10 ng/mL TNF-α for 24 h. **G**, total charge calculated from the integral of averaged amperometric currents in 3D acini control or 3D acini Syt-1-GFP with or without TNF-α incubation. **L**, number of dopamine molecules released toward the basal pole by 3D acini control or 3D acini Syt-1-GFP with or without TNF-α incubation. (*) $p < 0.05$ was considered significant.

3.2. Syt-1 overexpression increases exocytosis in the apical pole of 3D acini

To evaluate the effect of Syt-1 overexpression on exocytosis, HSG cells were transfected with Syt-1-GFP and then seeded on matrigel to form 3D acini, as previously described [22]. Syt-1 was endogenously expressed by both, 2D-culture and 3D acini, showing a dotted cytoplasmic pattern (Fig. 2A–C). Fig. 2D shows a Western blot with Syt-1 protein levels in 3D acini and 2D-culture with Syt-1-GFP or pEGFP-C1 vector transfection. Densitometric analysis of these immunoblots indicate that Syt-1 expression was significantly higher in Syt-1-GFP transfected cells compared with control cells, in both 3D acini and 2D-culture (Fig. 2D) ($p = 0.015$ and $p = 0.014$, respectively). Moreover, GFP showed a dotted cytoplasmic distribution in Syt-1-GFP transfected 3D acini and 2D-culture (Fig. 2F–H), similar to the basal distribution of endogenous Syt-1 (Fig. 2A–C).

Syt-1 regulates the overall rate of exocytosis and the stability of the

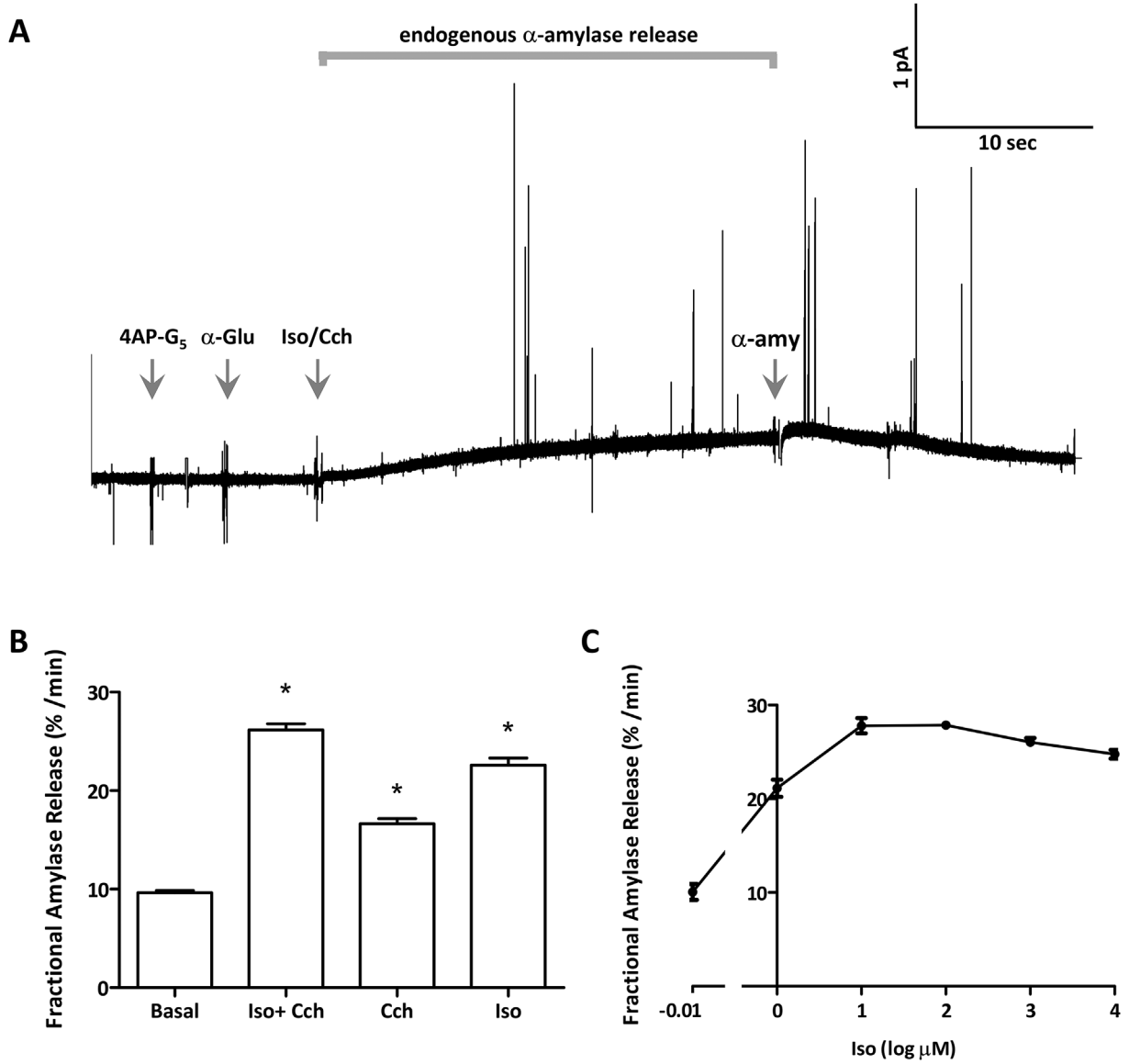

Fig. 4. Detection of endogenous α-amylase release and activity by 3D acini. **A**, current trace for carbon fiber electrode held at +150 mV with respect to the bath and positioned near the top of a 3D acinus. Small current artifacts and arrows indicate time of addition for the different agonists and substrates sequentially applied to the bath, 4-aminofenil-α-maltopentoside (6.5 mM), α-glucosidase (12.5 U/mL), Iso (10 μM), Cch (10 μM), α-amylase (2 U/ml). Large positive transients correspond to the electrochemical oxidation of 4AP originated from endogenous α-amylase modification of 4AP-G_5 after secretagogue stimulation. The addition of exogenous α-amylase was used as an enzymatic positive control. **B**, summary for the relative amount of amylase released under 10 μM Cch and/or 10 μM Iso added to the bath. **C**, Isoproterenol dose response for α-amylase release (as percentage of total) by 3D acini, (*) $p < 0.05$ was considered significant.

fusion pore [10]. To evaluate the effect of Syt-1 overexpression on exocytosis, 3D acini were pre-loaded with dopamine and its release was measured by amperometric recordings in the apical pole, using a carbon fiber held +660 mV. A representative acinus highlighting the apical and basal pole where the electrode was placed is shown in Fig. 2H. The time-course of dopamine release shows several amperometric spikes reflecting vesicle fusion events after stimulation with 10 μM Cch and 10 μM Iso in control 3D acini (Fig. 2I). The number of detectable amperometric spikes in the apical pole was lower after secretagogue stimulation in Syt-1-GFP transfected 3D acini, but the magnitude of spikes was larger (Fig. 2J). The total charge and thus the number of dopamine molecules was calculated from the integral of averaged amperometric currents, showing that the exocytosis was significantly increased in the apical pole of Syt-1-GFP transfected 3D acini than control 3D acini (Fig. 2K and L). We conclude that Syt-1 overexpression increases the magnitude of apical exocytic events.

3.3. TNF-α stimulation increases exocytic events in the basal pole, which is further enhanced by Syt-1 overexpression

Epithelial cell polarity is established and maintained by both, cell-cell and cell-extracellular matrix (ECM) adhesions, including tight junctions and hemidesmosomes, respectively [31]. LSG from SS-patients show altered acinar cell polarity with presence of mucins in the ECM [7] and disruption of tight junction structure, reproduced *in vitro* by incubation of isolated control acini with TNF-α or IFN-γ [5]. Based on these findings, the effect of TNF-α (1 or 10 ng/mL) on the exocytosis in the basal pole of control 3D acini or 3D acini overexpressing Syt-1 (3D acini Syt-1-GFP) was determined after loading with dopamine. No amperometric spikes were detected after Cch and Iso stimulation in the basal pole of 3D acini control and 3D acini Syt-1-GFP (Fig. 3A and B). Pre-treatment with TNF-α induced a concentration-dependent increase in the frequency of amperometric spikes in the basal pole after secretatogue stimuli (Fig. 3C–F). The total charge and the number of

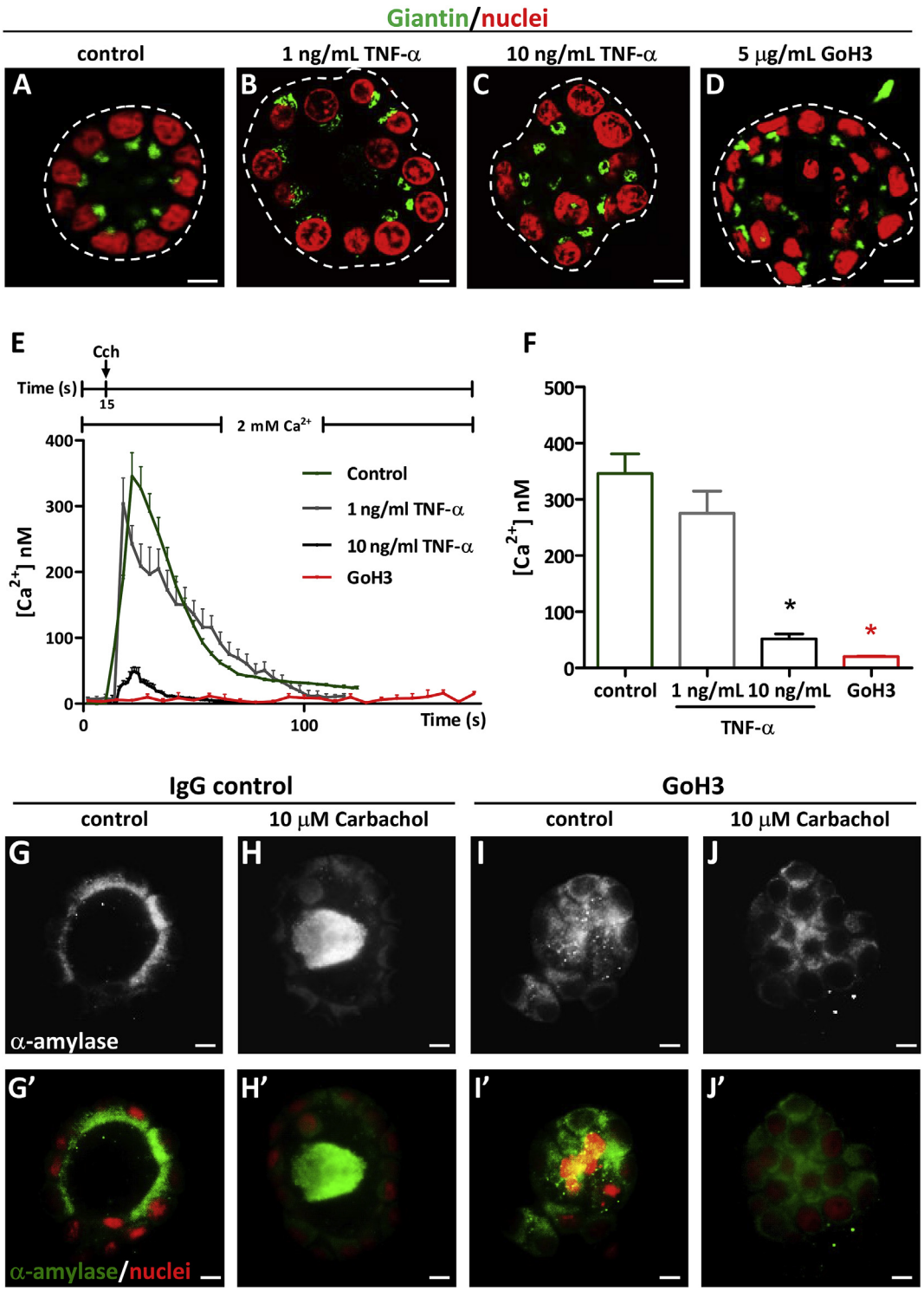

Fig. 5. Altered cell polarity affects Ca^{2+} signaling and amylase secretion in 3D acini. A-D, Giantin staining (green) in control and 3D acini incubated with 1 ng/mL TNF-α, 10 ng/mL TNF-α or 5 μg/mL GoH3 α6 integrin subunit -blocking antibody (used as polarity disrupting agents), bars: 10 μm. **E**, time course of free $[Ca^{2+}]_i$ detected with Fluo-4 after 10 μM Cch stimulation of control and 3D acini incubated with different concentrations of TNF-α or GoH3 antibody. **F**, quantification of cytoplasmic free $[Ca^{2+}]_i$ induced by Cch in control 3D acini and treated with TNF-α or GoH3 antibody. **G-H**, α-amylase staining (green) before and after 10 μM Cch stimulation in polarized 3D acini (treated with an irrelevant IgG), bars: 10 μm. **I-J**, α-amylase staining (green) before and after 10 μM Cch stimulation in 3D acini with altered cell polarity induced by GoH3 antibody, bars: 10 μm. (*) $p < 0.05$ was considered significant. (For interpretation of the references to colour in this figure legend, the reader is referred to the Web version of this article.)

dopamine molecules (calculated from the integral of averaged amperometric currents), showed that the magnitude of the exocytic events increased in the basal pole of 3D acini control after TNF-α stimulation, which was further enhanced in 3D acini Syt-1-GFP (Fig. 3G and H). Additionally, the stimulation of 3D acini with 1 or 10 ng/mL TNF-α induced an increase of Syt-1 and a decrease of SERCA2b mRNA levels (Supplementary Fig. 1D). These data suggest that TNF-α induces changes in the polarity of exocytic events.

3.4. Altered cell polarity affects the Ca^{2+} signaling and amylase secretion in 3D acini

LSG from SS-patients revealed disorganization of the ECM structure [32], with increased matrix metalloproteinase activity (towards fibronectin, laminin, and type IV collagen) [33] and altered expression and localization of α6β4 integrin [34], which altogether affect acinar cell polarity. In the present study, the amperometric recordings obtained from 3D acini show that endogenous α-amylase release is increased after secretagogue stimulation (Fig. 4A), of which a higher percentage is apparent after simultaneous stimulation by Cch and Iso (Fig. 4B). Also, a concentration-dependent increase after Iso stimulation saturates at a low agonist concentration (Fig. 4C), demonstrating that 3D acini are able to secrete α-amylase in response to cholinergic and adrenergic stimuli. Then, 3D acini cell polarity was disrupted *in vitro* with 1 or 10 ng/mL TNF-α for 24 h or 5 μg/mL GoH3, an α6 integrin subunit blocking antibody. Giantin (Golgi apparatus marker) presented supranuclear localization in the acinar cells of control 3D acini, while an altered distribution was detected in acinar cells after incubation with TNF-α or GoH3 antibody (Fig. 5A,–D). In these conditions, we noticed cytosolic Ca^{2+} ($[Ca^{2+}]_i$), evoked by 10 μM Cch in Fluo-4-loaded 3D acini, rapidly increased (Fig. 5E), reaching 346 ± 35 μM in control 3D acini (Fig. 5F). Moreover, $[Ca^{2+}]_i$ increase evoked by Cch was lower in 3D acini pre-treated with cell polarity disrupting agents (Fig. 5E), reaching 275.3 ± 39 μM after 1 ng/mL TNF-α, 51.85 ± 8 μM after 10 ng/mL TNF-α, and 19.30 ± 1 μM after GoH3 antibody incubation (Fig. 5F). Control 3D acini incubated with an irrelevant IgG synthesized α-amylase and then secreted towards the acinar lumen after 10 μM Cch stimulation (Fig. 5G and H). GoH3 incubation affected the secretory process, showing an accumulation of α-amylase in the cytoplasm of acinar cells (Fig. 5I and J). These results suggest that an altered cell polarity should have a significant effect over Ca^{2+} signaling and secretory events.

4. Discussion

The increased mRNA levels of Syt-1 found in this study validated our previous microarray data showing SYT1 among the top ranked differentially expressed genes in fractions enriched in epithelial cells of LSG from a different cohort of SS-patients [11]. Moreover, the incubation of 3D acini with TNF-α induced a concentration-dependent increase of Syt-1 mRNA levels, together with a significant decrease of SERCA2b mRNA levels (Supplementary Fig. 1). These findings resemble our observations *in vivo*, where Syt-1 mRNA and protein levels were found increased while SERCA2b levels were found decreased (Supplementary Fig. 1). It has been reported that the partial loss of SERCA2b affects the expression and activity of Ca^{2+} signaling proteins in the parotid gland acini of $SERCA2^{+/-}$ mice, increasing the expression of Syt-1 by a yet to be elucidated mechanism [35]. The *in silico* analysis of SYT1 promoter shows several response elements for transcription factors activated downstream pro-inflammatory cytokines, such as STAT1, STAT3, JUN, FOS, among others, suggesting that the chronic inflammation could induce the Syt-1 overexpression in SS-patients. Physiologically, the increase in $[Ca^{2+}]_i$ is achieved as a result of IP3R-mediated Ca^{2+} release from the endoplasmic reticulum and the Ca^{2+} entry into the acinar cells, both activated in response to stimulation of muscarinic or alpha-adrenergic receptors [36]. A change in the sensitivity of cells to acetylcholine (with attenuation of $[Ca^{2+}]_i$ increases and Ca^{2+}-dependent ion channel activation) was observed in isolated labial gland acinar cells from SS-patients compared to cells from healthy controls [37]. Teos et al. demonstrated that critical processes involved in fluid release such as Ca^{2+} release, Ca^{2+} entry, and cell volume reduction are altered in acinar cells from SS-patients. In addition, they associate the decrease in Ca^{2+} signaling in acinar cells to loss of IP3R2 and IP3R3, two critical IP3R subtypes in this gland [19]. Considering the aberrant Ca^{2+} signaling in acinar cells of LSG from SS-patients, Syt-1 overexpression could be a compensatory mechanism to improve the Ca^{2+} sensitivity thus increasing the probability of vesicle fusion.

The co-localization of Syt-1/STX4 and $PI(4,5)P_2$/Ezrin in the basolateral pole confirms the altered polarity of acinar cells of LSG from SS-patients and suggests the presence of functional fusion complexes that could allow the ectopic secretion of mucins towards the ECM [7]. It has been described that the exogenous delivery of $PI(4,5)P_2$ to the basal pole plasma membrane induced dramatic shrinkage of the lumen and re-localization of the apical markers GP135, Ezrin, and the tight junction component ZO-1, from the apical to the basolateral region [13]. Immunofluorescence and immunogold analysis have shown Ezrin primarily associated with the apical microvilli in LSG from control samples, while in SS-patients higher basal cytoplasm reactivity was observed [30]. In addition, in acini and ducts, ZO-1-specific staining of the apical plasma membrane was strongly diminished [5], suggesting that the apico-basal redistribution of $PI(4,5)P_2$ observed could have functional consequences in acinar cell polarity. Because $PI(4,5)P_2$ is a dominant phospholipid in the cytoplasmic leaflet at vesicle exocytic sites, Syt-1 interactions with $PI(4,5)P_2$ could mediate vectorial interactions between vesicle-tethered Syt-1 and plasma membrane sites for exocytosis [12]. Syt-1 promotes close membrane apposition by bridging the membranes allowing proximity of vesicle and plasma membrane SNARE proteins for complex assembly and fusion [12]. Our previous studies have shown a redistribution of STX4, STX3, SNAP-23 and VAMP8 from the apical to the basolateral pole, together with increased levels of preformed SNARE complexes [7]. These complexes are highly resistant to SDS solubilization, which prevents the formation of additional SNARE complex from free monomeric subunits after extraction [38]. Under similar experimental conditions, we observed a 100 kDa band for Syt-1 and an increase in the 100/65 kDa ratio in extract of LSG from SS-patients compared to controls, suggesting the presence of oligomers. Genetic analysis of Drosophila Syt-1 mutants has indicated that this protein functions in an oligomerized state [39]. In addition, Ca^{2+}-independent oligomerization of Syt-1 is crucial for rapid Ca^{2+}-dependent clustering via the C2B domain in response to Ca^{2+} influx through voltage-gated Ca^{2+} channels during neurotransmitter release [40]. This suggests a simple physical mechanism for regulation of exocytosis, where this oligomerization might serve as a platform organizing multiple SNAREpins to cooperatively open the fusion pore more swiftly [9]. PC12 cells overexpressing Syt-1 showed both altered exocytosis rate together with fusion pore stability [10]. Keeping in mind the pivotal role played by Syt-1 during exocytosis and its higher levels in LSG from SS-patients, overexpression demonstrated an increase in exocytic events in the acinar cell apical pole of 3D acini. However, the combined effect of TNF-α-induced cell polarity perturbation and Syt-1 overexpression elicit an increase in the frequency and magnitude of exocytic events in the basal pole, explained by an apico-basal redistribution of key components in this process and a higher Ca^{2+} sensitivity. Additionally, serum autoantibodies against M3 muscarinic receptors have been detected in SS-patients, showing inhibitory effects on parasympathetic neurotransmission [41], which could be associated with autonomic neuropathy in SS-patients [42]. There is no consensus that M3R autoantibodies are causative of the loss of salivary fluid secretion [18], however, these autoantibodies could decrease the acinar cell response to neural stimulation and lead to the glandular hypofunction [19]. In this context, the increase of Syt-1 expression could be a compensatory mechanism to maintain the secretory function. A not evaluated aspect in this work is the Syt-1 function in the nervous system of SS-patients, since it plays a key role during synaptic transmission, where the presynaptic vesicles fuse with the plasma membrane, releasing their neurotransmitters to activate postsynaptic receptors. It is known the synaptotagmins act as Ca^{2+} sensors to release and inhibit spontaneous fusion of synaptic vesicles in the absence of an action potential. Thus, synaptotagmins coordinate multiple stages of Ca^{2+}-triggered exocytosis, ensuring fast synaptic transmission for rapid information transfer

between neurons at synapses [43]. This is relevant topic considering the wide spectrum of peripheral polyneuropathy (PNP) or central nervous system affection in SS-patients, where 8.5–67% complain about neurological symptoms [42], including mono and polyneuropathy, cognitive dysfunction, mood disorders, anxiety disorders, cranial neuropathy and seizure disorders [44]. Anti-TNF agents (Infliximab and Etanercept) and B cell targeted therapies (Rituximab and Epratuzumab) have been used in primary SS, although no efficacy was found on neurological manifestations [45,46], which could be explained by the high and simultaneous number of altered biological processes occurring in the affected organs, just to mention as example, disturbances of the response to misfolded/unfolded proteins [22,47–49].

The spatiotemporal regulation of Ca^{2+} signals in SG acinar cells show that the first increase occurs by its release via the IP3R at the apical pole whilst entry channels (Orai 1 and TRPC1) contribute to the global spread of Ca^{2+} to basal region [14]. Here, secretagogue stimulation induced a fast and transient increase of $[Ca^{2+}]_i$ in control 3D acini although when pre-treated with TNF-α or α6 integrin subunit blocking antibody (polarity disrupting agents) a lower $[Ca^{2+}]_i$ together with altered endogenous α-amylase secretion was observed. It should be noted that the correct interaction between α6β4 integrin and laminins from plasma membrane and basal lamina, respectively, influences the establishment of a functional epithelial cell polarity [31]. In SS, the basal lamina of acini and ducts show a structural disorganization including laminin and collagen IV decrease [32] coupled with aberrant expression and localization of α6β4 integrin [34], suggesting changes in integrin/laminin interaction account for loss of structural integrity and cell polarity, resembled here in 3D acini incubated with α6 integrin subunit blocking antibody.

Moreover the overexpression of Syt-1 was significantly associated with parameters of salivary gland alterations, which suggest that the secretory dysfunction in salivary glands of SS-patients is associated to altered expression and/or localization of secretory machinery components [4,6,7] with additional altered epithelial cell polarity [5]. In this scenario, the present study has wider scope by combining cellular and molecular biology with electrophysiological approaches to demonstrate that Syt-1 overexpression increases the magnitude of exocytic events and TNF-α stimulation alters the vectoriality of the secretory process. These findings reveal the mechanism explaining the presence of ectopic secretory products in the ECM of LSG from SS-patients [7], demonstrated to be inducers of inflammation [8]. Knowledge about the cellular and molecular biology of epithelial cells of salivary glands in SS-patients undoubtedly leads us knowing in depth their alterations and this should be one of the platforms to find therapeutic strategies.

Funding

This work was supported by FONDECYT [1160015 and 1120062 to MJG, SA, CM, SG and IC] Fondecyt-Iniciación [11170049 to IC], Fondecyt-Postdoctoral [3170023 to MJB], and PhD fellowship Conicyt-Chile to JC, MB, HU and MJB.

Disclosure statement

The authors declare no conflicts of interest.

Author contributions

All authors were involved in drafting the article or revising it critically for important intellectual content, and all authors approved the final version to be published. María-Julieta González had full access to all of the data in the study and takes responsibility for the integrity of the data and the accuracy of the data analysis.

Study conception and design: J. Cortés, J. Hidalgo, I. Castro, M. Brito, H. Urra, P. Pérez, María-Julieta González.

Acquisition of data: J. Cortés, J. Hidalgo, S. Aguilera, I. Castro, M. Brito, H. Urra, P. Pérez, M-J. Barrera, P. Carvajal, S. González, C. Molina, V. Bahamondes, María-Julieta González.

Analysis and interpretation of data: J. Cortés, J. Hidalgo, I. Castro, M. Brito, H. Urra, P. Pérez, M-J. Barrera, U. Urzúa, S. González, C. Molina, V. Bahamondes, M. Hermoso, María-Julieta González.

Acknowledgements

We thank all the patients who participated in this study and gratefully acknowledge Professor Indu Ambudkar (Secretory Physiology Section, Molecular Physiology and Therapeutics Branch, National Institute of Dental and Craniofacial Research, National Institutes of Health, Bethesda, MD, USA) for assistance with calcium experiments and Dr Ilias Alevizos (Oral Medicine, National Institute of Dental and Craniofacial Research, NIH, Bethesda, MD, USA) for the help with overexpression experiments, Professor Arnoud Sonnenberg (Division of Cell Biology, The Netherlands Cancer Institute, The Netherlands) for providing the rat monoclonal antibody against the α6 integrin subunit (GoH3) and Professor Matthew Hoffman (Matrix and Morphogenesis Section, National Institute of Dental and Craniofacial Research, National Institutes of Health, DHHS, Bethesda, Maryland, USA) for providing growth factor-reduced Matrigel (BD Biosciences, San Jose, CA). We would also like to thank David Cox for his editing contribution.

Appendix A. Supplementary data

Supplementary data to this article can be found online at https://doi.org/10.1016/j.jaut.2018.10.019.

References

[1] I. Castro, D. Sepulveda, J. Cortes, A.F. Quest, M.J. Barrera, V. Bahamondes, et al., Oral dryness in Sjogren's syndrome patients. Not just a question of water, Autoimmun. Rev. 12 (2013) 567–574.
[2] M.N. Manoussakis, E.K. Kapsogeorgou, The role of intrinsic epithelial activation in the pathogenesis of Sjögren's syndrome, J. Autoimmun. 35 (2010) 219–224.
[3] P.C. Fox, M. Brennan, P. Di Sun, Cytokine expression in human labial minor salivary gland epithelial cells in health and disease, Arch. Oral Biol. 44 (Suppl 1) (1999) S49–S52.
[4] M.J. Barrera, V. Bahamondes, D. Sepúlveda, A.F. Quest, I. Castro, J. Cortés, et al., Sjögren's syndrome and the epithelial target: a comprehensive review, J. Autoimmun. 42 (2013) 7–18.
[5] P. Ewert, S. Aguilera, C. Alliende, Y.J. Kwon, A. Albornoz, C. Molina, et al., Disruption of tight junction structure in salivary glands from Sjögren's syndrome patients is linked to proinflammatory cytokine exposure, Arthritis Rheum. 62 (2010) 1280–1289.
[6] V. Bahamondes, A. Albornoz, S. Aguilera, C. Alliende, C. Molina, I. Castro, et al., Changes in Rab3D expression and distribution in the acini of Sjögren's syndrome patients are associated with loss of cell polarity and secretory dysfunction, Arthritis Rheum. 63 (2011) 3126–3135.
[7] M.J. Barrera, M. Sánchez, S. Aguilera, C. Alliende, V. Bahamondes, C. Molina, et al., Aberrant localization of fusion receptors involved in regulated exocytosis in salivary glands of Sjögren's syndrome patients is linked to ectopic mucin secretion, J. Autoimmun. 39 (2012) 83–92.
[8] M.J. Barrera, S. Aguilera, E. Veerman, A.F. Quest, D. Díaz-Jiménez, U. Urzúa, et al., Salivary mucins induce a Toll-like receptor 4-mediated pro-inflammatory response in human submandibular salivary cells: are mucins involved in Sjögren's syndrome? Rheumatology (Oxford) 54 (2015) 1518–1527.
[9] J. Wang, F. Li, O.D. Bello, C.V. Sindelar, F. Pincet, S.S. Krishnakumar, et al., Circular oligomerization is an intrinsic property of synaptotagmin, Elife 6 (2017).
[10] Z. Zhang, E. Hui, E.R. Chapman, M.B. Jackson, Regulation of exocytosis and fusion pores by synaptotagmin-effector interactions, Mol. Biol. Cell 21 (2010) 2821–2831.
[11] P. Pérez, J.M. Anaya, S. Aguilera, U. Urzúa, D. Munroe, C. Molina, et al., Gene expression and chromosomal location for susceptibility to Sjögren's syndrome, J. Autoimmun. 33 (2009) 99–108.
[12] T.F. Martin, PI(4,5)P_2-binding effector proteins for vesicle exocytosis, Biochim. Biophys. Acta 1851 (2015) 785–793.
[13] F. Martin-Belmonte, A. Gassama, A. Datta, W. Yu, U. Rescher, V. Gerke, et al., PTEN-mediated apical segregation of phosphoinositides controls epithelial morphogenesis through Cdc 42, Cell 128 (2007) 383–397.
[14] I.S. Ambudkar, Ca^{2+} signaling and regulation of fluid secretion in salivary gland acinar cells, Cell Calcium 55 (2014) 297–305.
[15] J.E. Melvin, D. Yule, T. Shuttleworth, T. Begenisich, Regulation of fluid and electrolyte secretion in salivary gland acinar cells, Annu. Rev. Physiol. 67 (2005) 445–469.

[16] J. Han, K. Pluhackova, R.A. Böckmann, The multifaceted role of SNARE proteins in membrane fusion, Front. Physiol. 8 (2017) 5.
[17] S.W. Messenger, M.A. Falkowski, G.E. Groblewski, Ca^{2+}-regulated secretory granule exocytosis in pancreatic and parotid acinar cells, Cell Calcium 55 (2014) 369–375.
[18] I. Ambudkar, Calcium signaling defects underlying salivary gland dysfunction, Biochim. Biophys. Acta. Mol Cell Res. (2018 Jul 10), https://doi.org/10.1016/j.bbamcr.2018.07.002 pii: S0167-4889(18)30148-4. [Epub ahead of print].
[19] L.Y. Teos, Y. Zhang, A.P. Cotrim, W. Swaim, J.H. Won, J. Ambrus, et al., IP3R deficit underlies loss of salivary fluid secretion in Sjögren's Syndrome, Sci. Rep. 5 (2015) 13953.
[20] C. Vitali, S. Bombardieri, R. Jonsson, H.M. Moutsopoulos, E.L. Alexander, S.E. Carsons, et al., Classification criteria for Sjögren's syndrome: a revised version of the European criteria proposed by the American-European Consensus Group, Ann. Rheum. Dis. 61 (2002) 554–558.
[21] T.E. Daniels, Labial salivary gland biopsy in Sjögren's syndrome. Assessment as a diagnostic criterion in 362 suspected cases, Arthritis Rheum. 27 (1984) 147–156.
[22] M.J. Barrera, S. Aguilera, I. Castro, J. Cortés, V. Bahamondes, A.F. Quest, et al., Pro-inflammatory cytokines enhance ERAD and ATF6α pathway activity in salivary glands of Sjögren's syndrome patients, J. Autoimmun. 75 (2016) 68–81.
[23] Y.J. Kwon, P. Pérez, S. Aguilera, C. Molina, L. Leyton, C. Alliende, et al., Involvement of specific laminins and nidogens in the active remodeling of the basal lamina of labial salivary glands from patients with Sjögren's syndrome, Arthritis Rheum. 54 (2006) 3465–3475.
[24] M.W. Pfaffl, G.W. Horgan, L. Dempfle, Relative expression software tool (REST) for group-wise comparison and statistical analysis of relative expression results in real-time PCR, Nucleic Acids Res. 30 (2002) e36.
[25] M.M. Bradford, A rapid and sensitive method for the quantitation of microgram quantities of protein utilizing the principle of protein-dye binding, Anal. Biochem. 72 (1976) 248–254.
[26] M. Fukuda, E. Kanno, Y. Ogata, K. Mikoshiba, Mechanism of the SDS-resistant synaptotagmin clustering mediated by the cysteine cluster at the interface between the transmembrane and spacer domains, J. Biol. Chem. 276 (2001) 40319–40325.
[27] J.M. Walker, The bicinchoninic acid (BCA) assay for protein quantitation, Methods Mol. Biol. 32 (1994) 5–8.
[28] M.J. Batchelor, S.C. Williams, M.J. Green, Amperometric determination of total amylase, J. Electroanal. Chem. Interfacial Electrochem. 246 (1988) 307–311.
[29] Y. Lai, X. Lou, J. Diao, Y.K. Shin, Molecular origins of synaptotagmin 1 activities on vesicle docking and fusion pore opening, Sci. Rep. 5 (2015) 9267.
[30] P. Pérez, S. Aguilera, N. Olea, C. Alliende, C. Molina, M. Brito, et al., Aberrant localization of ezrin correlates with salivary acini disorganization in Sjogren's Syndrome, Rheumatology (Oxford) 49 (2010) 915–923.
[31] W.J. Nelson, Epithelial cell polarity from the outside looking in, News Physiol. Sci. 18 (2003) 143–146.
[32] C. Molina, C. Alliende, S. Aguilera, Y.J. Kwon, L. Leyton, B. Martínez, et al., Basal lamina disorganisation of the acini and ducts of labial salivary glands from patients with Sjogren's syndrome: association with mononuclear cell infiltration, Ann. Rheum. Dis. 65 (2006) 178–183.
[33] E. Goicovich, C. Molina, P. Pérez, S. Aguilera, J. Fernández, N. Olea, et al., Enhanced degradation of proteins of the basal lamina and stroma by matrix metalloproteinases from the salivary glands of Sjögren's syndrome patients: correlation with reduced structural integrity of acini and ducts, Arthritis Rheum. 48 (2003) 2573–2584.
[34] J. Velozo, S. Aguilera, C. Alliende, P. Ewert, C. Molina, P. Pérez, et al., Severe alterations in expression and localisation of {alpha}6{beta}4 integrin in salivary gland acini from patients with Sjogren syndrome, Ann. Rheum. Dis. 68 (2009) 991–996.
[35] J.H. Choi, H. Jo, J.H. Hong, S.I. Lee, D.M. Shin, Alteration of expression of Ca2+ signaling proteins and adaptation of Ca2+ signaling in SERCA2+/- mouse parotid acini, Yonsei Med. J. 49 (2008) 311–321.
[36] I.S. Ambudkar, Calcium signalling in salivary gland physiology and dysfunction, J. Physiol. 594 (2016) 2813–2824.
[37] L.J. Dawson, E.A. Field, A.R. Harmer, P.M. Smith, Acetylcholine-evoked calcium mobilization and ion channel activation in human labial gland acinar cells from patients with primary Sjögren's syndrome, Clin. Exp. Immunol. 124 (2001) 480–485.
[38] L. Wang, M.A. Bittner, D. Axelrod, R.W. Holz, The structural and functional implications of linked SNARE motifs in SNAP25, Mol. Biol. Cell 19 (2008) 3944–3955.
[39] J.T. Littleton, H.J. Bellen, Synaptotagmin controls and modulates synaptic-vesicle fusion in a Ca(2+)-dependent manner, Trends Neurosci. 18 (1995) 177–183.
[40] M. Fukuda, K. Mikoshiba, Mechanism of the calcium-dependent multimerization of synaptotagmin VII mediated by its first and second C2 domains, J. Biol. Chem. 276 (2001) 27670–27676.
[41] S.A. Waterman, T.P. Gordon, M. Rischmueller, Inhibitory effects of muscarinic receptor autoantibodies on parasympathetic neurotransmission in Sjögren's syndrome, Arthritis Rheum. 43 (2000) 1647–1654.
[42] T. Gono, Y. Kawaguchi, Y. Katsumata, K. Takagi, A. Tochimoto, S. Baba, et al., Clinical manifestations of neurological involvement in primary Sjögren's syndrome, Clin. Rheumatol. 30 (2011) 485–490.
[43] T. Bacaj, D. Wu, J. Burré, R.C. Malenka, X. Liu, T.C. Südhof, Synaptotagmin-1 and -7 Are Redundantly Essential for Maintaining the Capacity of the Readily-Releasable Pool of Synaptic Vesicles, PLoS Biol. 13 (2015) e1002267.
[44] E. Harboe, A.B. Tjensvoll, S. Maroni, L.G. Gøransson, O.J. Greve, M.K. Beyer, et al., Neuropsychiatric syndromes in patients with systemic lupus erythematosus and primary Sjögren syndrome: a comparative population-based study, Ann. Rheum. Dis. 68 (2009) 1541–1546.
[45] A. Mekinian, P. Ravaud, C. Larroche, E. Hachulla, B. Gombert, C. Blanchard-Delaunay, et al., Rituximab in central nervous system manifestations of patients with primary Sjögren's syndrome: results from the AIR registry, Clin. Exp. Rheumatol. 30 (2012) 208–212.
[46] S. Ozgocmen, A. Gur, Treatment of central nervous system involvement associated with primary Sjögren's syndrome, Curr. Pharmaceut. Des. 14 (2008) 1270–1273.
[47] D. Sepúlveda, M.J. Barrera, I. Castro, S. Aguilera, P. Carvajal, C. Lagos, et al., Impaired IRE1α/XBP-1 pathway associated to DNA methylation might contribute to salivary gland dysfunction in Sjögren's syndrome patients, Rheumatology (Oxford) 57 (2018) 1021–1032.
[48] M.J. Barrera, S. Aguilera, I. Castro, S. González, P. Carvajal, C. Molina, et al., Endoplasmic reticulum stress in autoimmune diseases: can altered protein quality control and/or unfolded protein response contribute to autoimmunity? A critical review on Sjögren's syndrome, Autoimmun. Rev. 17 (2018) 796–808.
[49] C. Lagos, P. Carvajal, I. Castro, D. Jara, S. González, S. Aguilera, et al., Association of high 5-hydroxymethylcytosine levels with Ten Eleven Translocation 2 over-expression and inflammation in Sjögren's syndrome patients, Clin. Immunol. (2018 Jun 9), https://doi.org/10.1016/j.clim.2018.06.002 pii: S1521-6616(18)30348-6. [Epub ahead of print].